

Northumbria Research Link

Citation: Rutter, Nick, Marshall, Hans-Peter, Tape, Ken and Essery, Richard (2010) Observations of snowpack properties to evaluate ground-based microwave remote sensing. In: BHS 2010 International Symposium: Managing Consequences of a Changing Global Environment, 19th - 23rd July 2010, Newcastle upon Tyne.

URL:

This version was downloaded from Northumbria Research Link:
<https://nrl.northumbria.ac.uk/id/eprint/21391/>

Northumbria University has developed Northumbria Research Link (NRL) to enable users to access the University's research output. Copyright © and moral rights for items on NRL are retained by the individual author(s) and/or other copyright owners. Single copies of full items can be reproduced, displayed or performed, and given to third parties in any format or medium for personal research or study, educational, or not-for-profit purposes without prior permission or charge, provided the authors, title and full bibliographic details are given, as well as a hyperlink and/or URL to the original metadata page. The content must not be changed in any way. Full items must not be sold commercially in any format or medium without formal permission of the copyright holder. The full policy is available online: <http://nrl.northumbria.ac.uk/policies.html>

This document may differ from the final, published version of the research and has been made available online in accordance with publisher policies. To read and/or cite from the published version of the research, please visit the publisher's website (a subscription may be required.)

Observations of snowpack properties to evaluate ground-based microwave remote sensing

Nick Rutter¹, Hans-Peter Marshall², Ken Tape³ and Richard Essery⁴

¹School of Applied Sciences, Northumbria University, UK; ²Center for Geophysical Investigation of the Shallow Subsurface, Boise State University, USA;

³Institute of Arctic Biology, University of Alaska Fairbanks, Fairbanks, USA; ⁴School of GeoSciences, University of Edinburgh, UK

Email: nick.rutter@northumbria.ac.uk

Abstract

Active microwave radar has been shown to have great potential for estimating snow water equivalent (SWE) globally from space. To help evaluate optimal active microwave sensor configurations to observe SWE, we evaluated ground-based Frequency Modulated Continuous Wave (FMCW) radar (12–18 GHz, cross-polarisation) using very high resolution *in-situ* observations of snowpack layering, dielectric permittivity and density over a 10 m snow trench on Toolik Lake, Alaska. Results showed that the thicknesses of layers within the 10 m trench were highly variable over short distances (< 1 m), even where total snow depth changed very little. Layer boundaries observed using NIR photography identified all bands of high radar backscatter. Although additional observations of density and dielectric permittivity helped to explain the causes of backscatter, not all snowpack properties which cause backscatter were coincident with strong vertical changes in density or permittivity. Further observations of high surface roughness in layer boundaries explained some areas of weak backscatter, nonetheless it was shown that a suite of coincident observations, rather than a single technique in isolation, were required to adequately explain the variability of backscatter and the influence of snowpack properties upon it.

Introduction

Successive discrete precipitation events throughout a winter accumulate to form layered snowpacks. Between precipitation events, compaction, metamorphism (temperature gradient and isothermal), melt, refreeze and redistribution of snow by wind (both scour and deposition), all impact on the internal snowpack layering. Consequently, a single vertical snowpack profile, which documents distinct differences in physical properties of each layer, acts as a record of the hydrometeorological history of the winter.

Variability of snowpack properties between layers are often much greater than the variability of properties within layers. However, the horizontal extent and vertical thickness of individual layers can be highly heterogeneous, especially in tundra environments. Sturm and Benson (2004) show that layering extent can be discontinuous over short (<1 m) spatial scales and highly variable in the vertical axis; layer boundaries within a snowpack can therefore be far rougher than the surface-air boundary. Where the differences in layer densities are large and thickness of layers are highly variable, horizontal changes in snow water equivalent (SWE) can be large despite the variability of total snow depth being low. Also, when there are strong differences between the microstructure and permittivity of adjacent layers, the proportion and position in the vertical profile of each layer type relative to total snow depth and the roughness of each layer boundary has big implications for estimates of volume scattering and backscatter, for both passive and active microwave remote sensing as well as radiative transfer modelling (Durand *et al.*, 2008).

As current operational microwave satellites do not have optimal sensor configurations to observe SWE, field campaigns that use airborne and ground-based radars and radiometers to evaluate potential future sensor configurations

have become increasingly prevalent (Yueh *et al.*, 2007; Hardy *et al.*, 2008; Cline *et al.*, 2009). In such field campaigns, the need to be able to observe the variability of SWE, layering and other physical properties of the snowpack (e.g. microstructure and dielectric permittivity) within footprints of airborne and especially ground-based sensors is of great importance to enable understanding of variability in scattering of microwave energy. To achieve the resolution required to adequately evaluate ground-based microwave sensors, Tape *et al.* (2010) detail recent developments in the application of near-infrared (NIR) photography that allow layer boundaries within tundra snowpacks to be observed at the centimetre scale over large horizontal extents (10 m). This allows optimal evaluation of microwave sensors which have wavelengths on the order of the centimetre scale (i.e. Ku-band; $\lambda = 1.67\text{--}2.5$ cm). Although the footprint extent of ground-based microwave sensors depends on the exact configuration of antenna pattern, frequency, as well as the distance and angle between the sensor and the snow surface, 10 m is generally sufficient to capture multiple radar or radiometer observations.

In this paper we evaluate ground-based Frequency Modulated Continuous Wave (FMCW) radar using very high resolution *in-situ* observations of snowpack layering (i.e. snowpack stratigraphy), dielectric properties and density; collected in February 2008 on Toolik Lake, Alaska, as part of the NASA Cold Land Processes Experiment (CLPX) II. Areas of high and low intensity radar backscatter along a 10 m trench are compared with internal layer boundaries, the roughness of each boundary, as well as major contrasts in density and dielectric permittivity.

Methods

Toolik Lake (68°38'N, 149°36'W) is situated on the North

Slope of Alaska, USA. On 23 February 2008 a 10 m transect in a snowdrift was marked out perpendicular to the edge of the north side of the lake extending out from the shore onto lake ice. The lake ice was frozen to the bed throughout the length of the trench.

A FMCW radar (12–18 GHz, cross-polarisation) was mounted in a nadir position off a horizontal cross-arm attached to freely moving sled. The broad bandwidth of the radar allowed a resolution of ~ 1 cm in snow. The sled was very slowly winched (< 2 cm s^{-1}) along the transect whilst recording radar backscatter 40 times a second. Differential GPS (Trimble 5700) was used to geo-locate the position of the sled, and therefore each radar trace, along the transect to an absolute accuracy of < 5 cm. The nominal footprint size of the radar was 50×50 cm.

Once the radar measurements were made, a 10 m trench was excavated along the centre line of the radar footprint. The face of the trench was cut with snow saws to be as near vertical as possible. Any artefacts resulting from the excavation process, for example teeth marks from the snow saws, were carefully removed using soft brushes and rounded wooden blocks. NIR photographs were taken of the trench face at ~ 35 cm intervals along the trench face, creating $\sim 30\%$ overlap between adjacent photographs. A detailed discussion of the measurement, post-processing and georeferencing protocols can be found in Tape *et al.* (2010). As a result, layers in georeferenced images along the 10 m trench face were visually identified at a 1 cm horizontal resolution. The thicknesses of each layer at a 1 cm horizontal resolution were calculated and two roughness indices were calculated for each layer boundary over a 50 cm horizontal moving window to replicate the footprint length of the radar. Roughness indices were determined following Fassnacht *et al.* (2009), where layers were first detrended to remove slope influences, then random roughness (RR), the standard deviation of the elevations from the mean surface, and the sum of the absolute slopes (RM) were both calculated for each 50 cm window.

Subsequent to NIR photography, coincident *in situ* observations of dielectric permittivity and density

were made. Observations of dielectric permittivity were made using a Finnish snow fork (Sihvola and Tiuri, 1986) at 50 cm horizontal and 5 cm vertical spacing. The snow fork was inserted horizontally into the snowpack and each measurement integrated over a volume $\sim \pm 2$ cm above and below the fork. Reliable observations of dielectric permittivity using a snow fork were not possible less than 5 cm away from the snow-air interface. Density observations were made using a 100 cm³ box-type cutter at 200 cm horizontal spacing within individual layers in the vertical dimension. Where possible, two density samples were taken in each layer at each of the six positions along the trench. However, due to limitations of layer thicknesses and the occasional inability to get a reliable sample from each position along the trench, between 4 and 12 density samples from taken in each layer throughout the trench. Visual assessments of snow type within each layer were made at 0, 5 and 9.5 m horizontally along the trench.

Results

In each image, layers were georegistered relative to a reference point, given by the tape measure in the horizontal and the ruler in the vertical (Figure 1). Although the lake ice surface was almost flat, it was not absolutely flat, so the vertical reference point for georegistering each individual image (where the base of the vertical ruler rests on the ice surface) varied between adjacent images due to localised ice roughness. Consequently, when layer boundaries identified in adjacent images were concatenated together abrupt visual discontinuities were possible (see Figure 2a) where adjacent images met. However, when adjacent images were aligned to a well defined boundary (e.g. the surface-air boundary) almost all of the abrupt discontinuities in layer boundaries were removed (Figure 2b). Discontinuities that remained were a function of visual misclassification during layer identification. Although such discontinuities introduced slight errors into subsequent roughness analysis, the potential maximum number of discontinuities is less than 1% of the

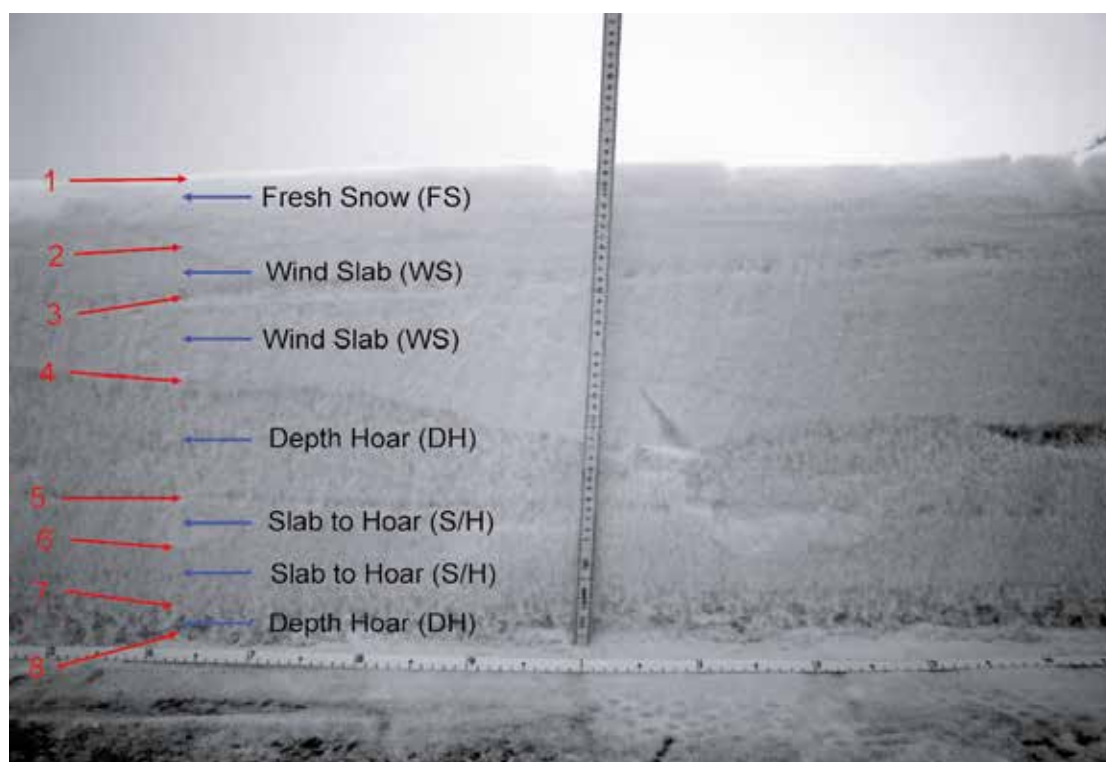


Figure 1 Example NIR image of trench section; annotated with layer boundaries and snow types.

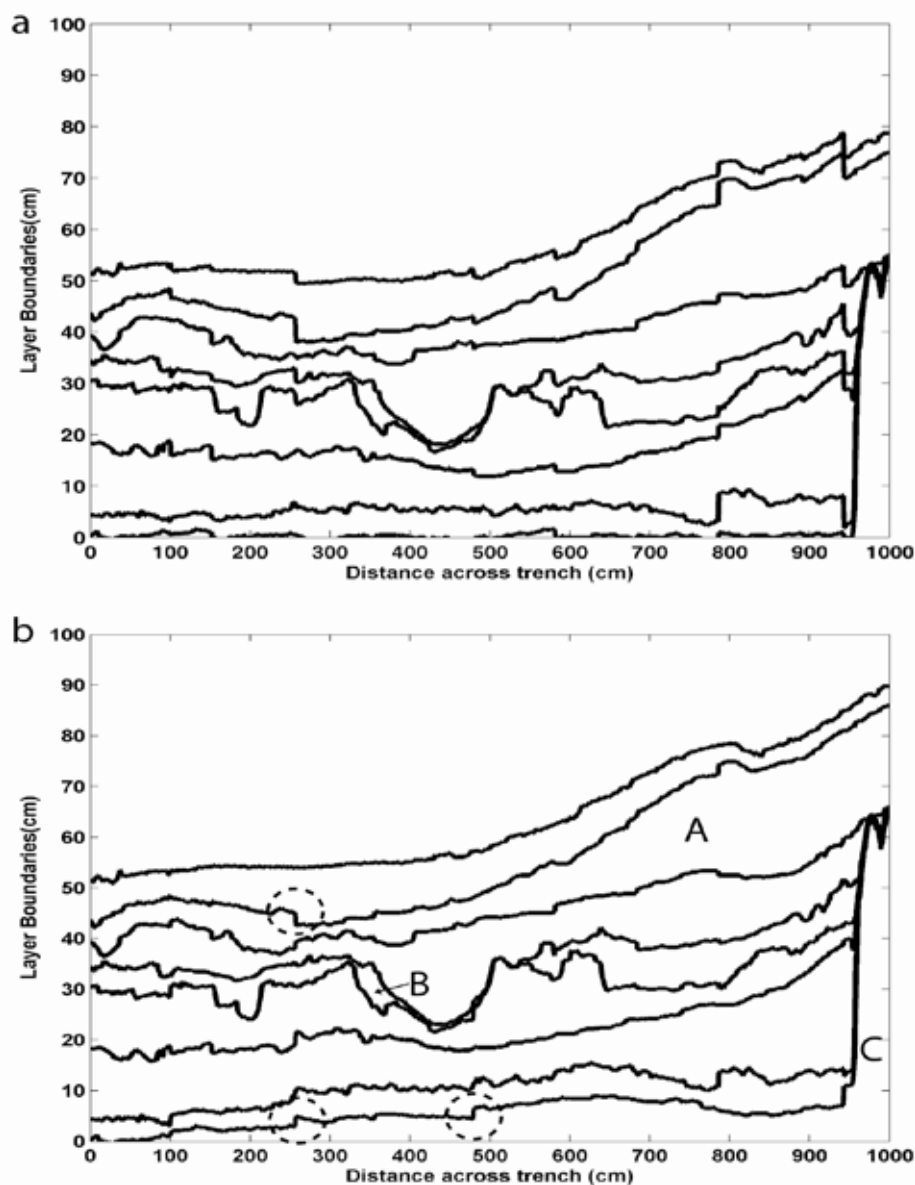


Figure 2 (a) Snowpack layer boundaries (including surface and base) determined directly from adjacent NIR images. (b) as (a) except the snow-air boundary was used as a reference point with which to align adjacent images (see text for further description).

total number of observations, and in reality only a small proportion of these were visually obvious (dashed circles highlight three examples in Figure 2b). For analysis of layer boundary roughness, observations aligned to the snow-air interface were used (i.e. Figure 2b). For comparison of layer boundaries with radar, density and dielectric permittivity, all of which were not adjusted in the same manner, unaligned observations were used (Figure 2a).

Eight layer boundaries, including the snow-air and snow-lake ice boundaries, were evident across the 10 m trench. Figure 1 highlighted these boundaries in a random vertical profile and attributed a snow type to each layer, which were consistent throughout each layer across the trench. Figure 2b indicated that the thickness of all layers did not increase equally as total snow depth increased with distance across the trench. Some layers increased in thickness (A in Figure 2b), while other layers pinched out and re-emerged (B in Figure 2b). A large rock on the edge of the lake shore was the cause of the rapid decrease in thickness of lower layers from ~950 cm onwards (C in Figure 2b). Figure 2b clearly showed that some layers were highly variable throughout the trench (e.g. the upper depth hoar layer between boundaries 4 and 5) whereas others were not (e.g. fresh snow between boundaries 1 and 2).

Two major bands of backscatter that had a high degree of coherency in the horizontal direction were evident

around the snow-air and snow-lake ice boundary interfaces (Figure 3). Three further bands of backscatter were evident within the snowpack, although with far less horizontal coherency. Layer boundaries identified using NIR images were coincident with these bands of backscatter. Steep vertical gradients in backscatter followed the upper and lower boundaries of the fresh snow layer and the lower depth hoar layer, enclosing bands of high backscatter within. Layer boundary 3 followed the mid-point of a discontinuous band of backscatter between wind slab layers that was most coherent between 0–500 cm, but was still recognisable up to 950 cm. Areas of high radar backscatter were coincident, albeit even less coherent, with layer boundary 5. A similar degree of horizontal coherency in radar backscatter was evident around layer boundary 6, particularly between 0–500 cm. From 650–950 cm layers 5 and 6 appeared to delimit upper and lower bounds of a discontinuous region of high backscatter.

Differences in density between adjacent layers, shown in Figure 4a, are significantly different when the whiskers of the box plots do not overlap. Such differences were evident at layer boundaries 2, 4, 5 and 7, when boxplot whiskers which delimit 1.5 of the interquartile range below the lower quartile and above the upper quartile did not overlap (Figure 4a). These boundaries, highlighted in Figure 4b, picked out the internal snowpack layer boundaries around the most horizontally coherent bands of backscatter

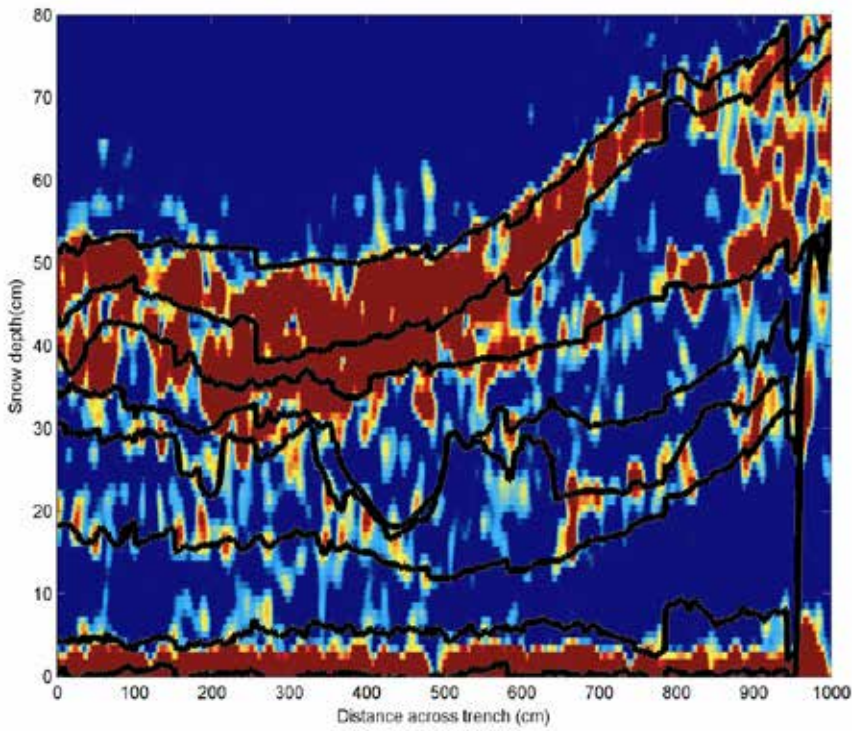


Figure 3 FMCW backscatter plot (warm colours are areas of high backscatter; cool colours are areas of low backscatter) with NIR layer boundaries (unaligned) overlaid.

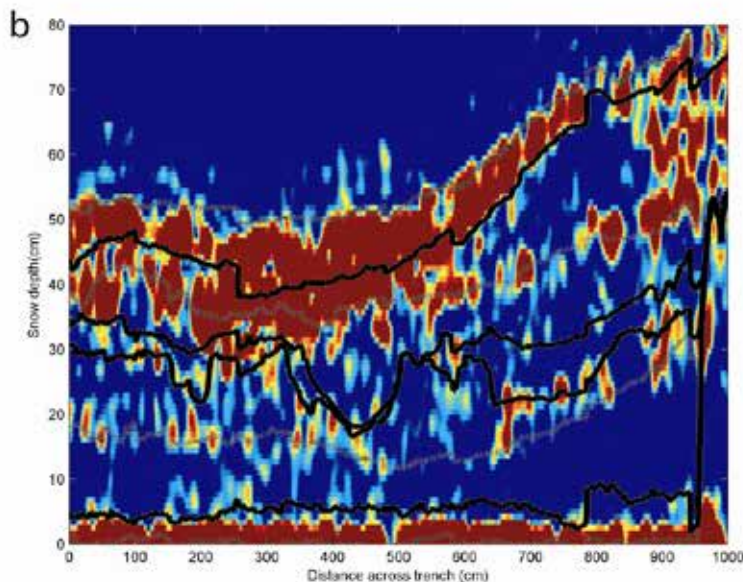
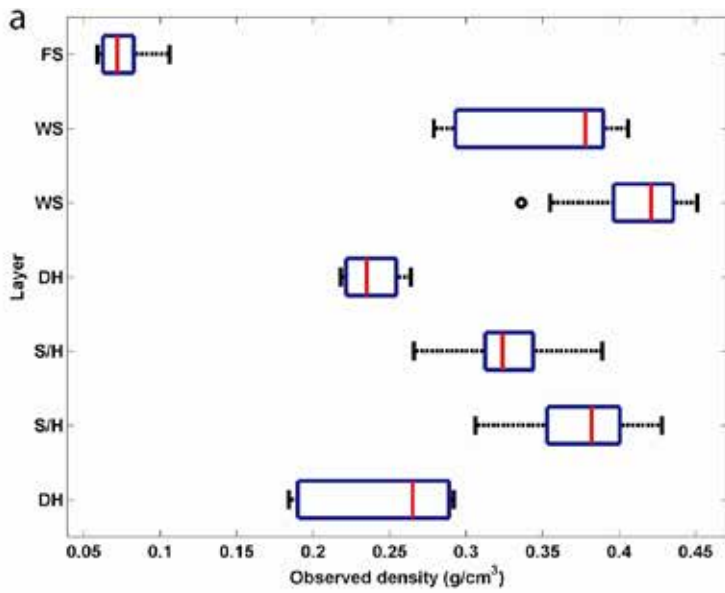


Figure 4 (a) Boxplots describing the distribution of density observations in each layer (whisker length is 1.5 of the inter-quartile range, circles are outliers beyond this range). Layer identifiers are given in Figure 2. (b) FMCW backscatter plot (warm colours are areas of high backscatter; cool colours are areas of low backscatter) with NIR layer boundaries (unaligned) overlaid. Solid black lines reflect internal snowpack boundaries between densities that were significantly different from each other, otherwise lines are dotted grey.

(beneath fresh snow and above lower depth hoar). However, the only other large density change that was coincident with a discontinuous band of backscatter was around possibly the least coherent backscatter band associated with layer boundary 5. Other more coherent internal backscatter bands, coincident with layer boundaries 3 and 6, were not identified by changes in layer density.

Two horizontal bands, between 5–25 cm and 30–60 cm snow depth, of relatively high dielectric permittivity were present throughout the trench (Figure 5a).

Horizontal discontinuities occurred in the upper band between 300–400 cm and in the lower band between 500–600 cm. Vertical gradients in permittivity were steepest around the edges of the upper band, which were broadly coincident with layer boundaries 2 and 4; a weaker vertical gradient around the upper edge of the lower band was broadly coincident with layer boundary 6 (Figure 5a). Layer boundaries 2 and 4 were coincident with the upper and lower limits of the wind slab layers. In comparison with radar backscatter (Figure 5b), layer boundary 2 was coincident with a strong vertical gradient in backscatter on the upper boundary of the wind slab. Layer boundary 4 was coincident with a weak backscatter band between 400–950 cm, which was more discontinuous than between 0–450 cm throughout which layer boundary 4 was not coincident. Layer boundary 6, between the two slab to hoar layers, was coincident with a discontinuous band of

radar backscatter, but the other coherent internal backscatter band, coincident with layer boundary 3, was not identified by changes in dielectric permittivity.

Two indices describing the roughness of layer boundaries (Figure 6a and 6b) indicated that up to 950 cm, before the rock strongly influenced roughness, boundary layers 4 and 5 were the only layers that peaked in roughness ($RR > 2$; $RM > 10$) above background fluctuations. Layer boundary 5 had the highest roughness indices and peaked four times throughout the length of the trench. Layer boundary 4 peaked with slightly lower roughness values in both indices at two of the four peaks highlighted by layer boundary 5. Both layer boundaries border the upper depth hoar layer, the rougher of the two boundaries being the lower border of that layer. The location of both boundary layers during peak roughness are coincident with areas where radar backscatter is low (Figure 6c), particularly around 500 cm and 650 cm, and less so around 175 cm and 350 cm.

Discussion and Conclusions

Near-infrared photography allowed rapid observations of high resolution layer boundary information at the same scale (~1 cm) as the wavelengths of the radar under evaluation. As a consequence, the heterogeneity of snowpack layering, and

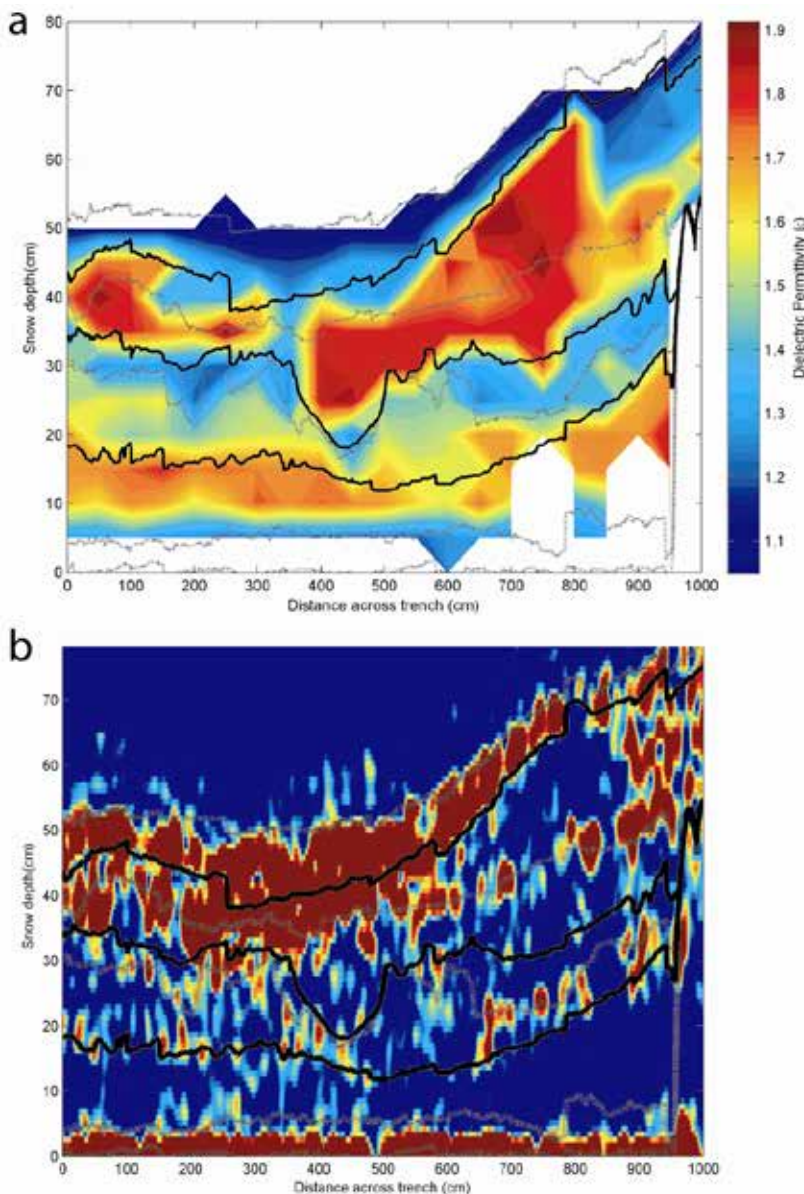


Figure 5 (a) Dielectric permittivities (a contour plot from a regular matrix of observations using 50 contour levels) with NIR layer boundaries (unaligned) overlaid. Solid black lines reflect internal snowpack boundaries that generally follow steep vertical gradients in permittivities, otherwise lines are dotted grey. (b) FMCW backscatter plot (warm colours are areas of high backscatter, cool colours are areas of low backscatter) with NIR layer boundaries (unaligned) overlaid as in (a).

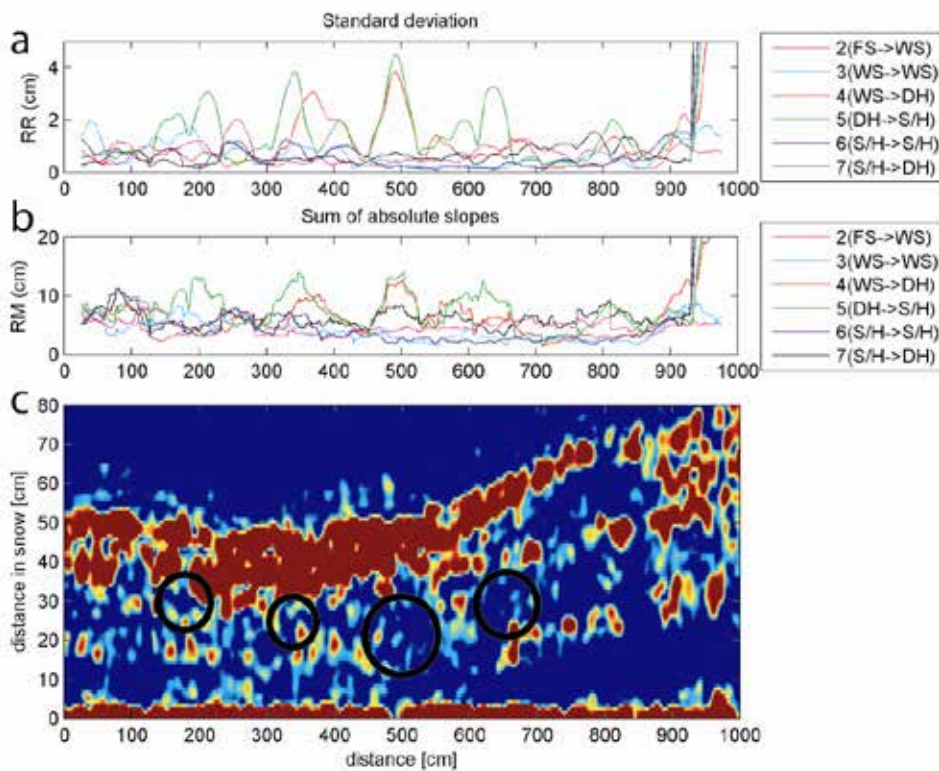


Figure 6 (a) Random roughness of each layer boundary (layer identifiers are given in Figure 2). (b) Sum of absolute slopes of each layer boundary. (c) FMCW backscatter plot (warm colours are areas of high backscatter, cool colours are areas of low backscatter) with black circles outlining the areas that correspond to the locations of boundary 4 and 5 where peaks were evident in (a) and (b).

to a certain extent the bulk differences in physical properties between layers, could for the first time be adequately quantified within the footprint of a ground-based radar.

In sections of the trench where the variability of total snow depth was low over short spatial scales (< 1 m), the variability of layer thicknesses within the same area of snowpack could be very high. Consequently the degree of radar backscatter would be hidden by simple analysis of total snow depth or SWE. Two examples within the trench illustrate this heterogeneity in layer thickness. Firstly, despite the lake ice-snowpack interface being almost flat the degree of layer thickness variability was high between boundaries 3 and 6 between 300 and 600 cm. Preferential scour of the structurally weak internal hoar layer in this area had been followed by subsequent deposition and compaction of snow in the scoured void and formed part of the overlying wind slab layer. This feature was independent of topography and resulted from a combination of spatially limited structural weakness and wind action. Secondly, when the total snow depth increased in the section of the trench between 600–950 cm, that increase was not applied equally across all layer thicknesses. Instead, the upper wind slab layer and the lower slab to hoar layer increased in thickness at the expense of all other layers, most likely due to localised increased slope angle and surface resistance of each layer causing preferential deposition of blowing snow.

High radar backscatter is a function of a change in the dielectric properties of the medium through which the energy is transmitted and the angle of interfaces relative to the angle of the antenna. Although both the density (indicative of the dielectric properties of each layer), as well as direct observations of the dielectric permittivity, highlighted the location of a number of the internal bands of backscatter, only the layer boundaries identified by NIR were coincident with all observed areas of backscatter within the snowpack (including the surface and base interfaces). Areas within layer boundaries where the surface roughness was high coincided visually with areas of low backscatter. However, not all areas of low backscatter, particularly in horizontally discontinuous internal bands of backscatter had a high roughness. Using the density and permittivity observations in conjunction

with NIR layer boundary identification allowed more about the causes of backscatter, or lack thereof, to be ascertained. Consequently, a suite of coincident observations such as those presented will allow an improved ability to evaluate new microwave sensor configurations and help constrain and improve inversion algorithms. In summary, from this study we conclude that:

1. Thicknesses of layers within snowpacks over arctic lake ice can be highly variable over short distances (< 1 m), even where total snow depth changes very little.
2. Layer variability resulting from expansion, contraction, pinching-out and reappearance are all in evidence throughout the 10 m.
3. Layer boundaries observed using NIR photography identify all bands of high radar backscatter.
4. Although density and dielectric permittivity observations aid the identification of backscatter and help explain their causes, not all snowpack properties which cause backscatter are coincident with strong vertical changes in density or permittivity.
5. Areas of high surface roughness of certain layer boundaries explain some areas of weak backscatter.
6. A suite of coincident observations, rather than a single technique in isolation, are required to adequately explain the variability of backscatter and the influence of snowpack properties upon it.

The methodology outlined by this study, and results from a single trench, provided the centimetre scale data required for a thorough evaluation of ground-based microwave sensors. However, as well as direct evaluation of coincident microwave measurements these data will enable future work to: (1) initialise retrieval algorithms (either as stand-alone simulations or linked to snowpack models), (2) understand the spatial variability of modelled backscatter within radar footprints, and (3) by degrading the information, understand the sensitivity of modelled backscatter to decreasing complexity in snowpack stratigraphy both in vertical and horizontal directions.

References

- Cline, D., Yueh, S., Chapman, B., Stankov, B., Gasiewski, A., Masters, D., Elder, K., Kelly, R., Painter, T.H., Miller, S., Katzberg, S. and Mahrt, L. 2009. NASA Cold Land Processes Experiment (CLPX 2002/03): airborne remote sensing. *J. Hydrometeorol.*, **10**, 338–346. 10.1175/2008jhm883.1.
- Durand, M., Kim, E.J. and Margulis, S.A. 2008. Quantifying Uncertainty in modeling snow microwave radiance for a mountain snowpack at the point-scale, including stratigraphic effects. *IEEE Trans. Geoscience and Remote Sensing* **46**, 1753–1767.
- Fassnacht, S.R., Stednick, J.D., Deems, J.S. and Corrao, M.V. 2009. Metrics for assessing snow surface roughness from digital imagery. *Water Resour. Res.*, **45(W00D31)**, 6. 10.1029/2008wr006986.
- Hardy, J., Davis, R., Koh, Y., Cline, D., Elder, K., Armstrong, R., Marshall, H.-P., Painter, T., Saint-Martin, G.C., DeRoo, R., Sarabandi, K., Graf, T., Koike, T. and McDonald, K. 2008. NASA Cold Land Processes Experiment (CLPX 2002/03): local scale observation Site. *J. Hydrometeorol.*, **9**, 1434–1442.
- Sihvola, A. and Tiuri, M. 1986. Snow fork for field determination of the density and wetness profiles of a snow pack. *IEEE Trans. Geoscience and Remote Sensing*, **24**, 717–721.
- Sturm, M. and Benson, C. 2004. Scales of spatial heterogeneity for perennial and seasonal snow layers. *Ann. Glaciol.*, **38**, 253–260.
- Tape, K.D., Rutter, N., Marshall, H.-P., Essery, R. and Sturm, M. 2010. Recording microscale variations in snowpack layering using near-infrared photography. *J. Glaciol.*, **56**, 75–80.
- Yueh, S., Cline, D. and Elder, K. 2007. Airborne Ku-band radar remote sensing of terrestrial snow cover. *IGARSS: 2007 IEEE Int. Geoscience and Remote Sensing Symp., Vols 1-12: Sensing and understanding our planet*, 1211–1214.